Commun. Theor. Phys. **72** (2020) 035003 (7pp) https://doi.org/10.1088/1572-9494/ab6908

Three-dimensional mixed convection flow with variable thermal conductivity and frictional heating

M Qasim[1,2,4], N Riaz[2], Dianchen Lu[1] and S Shafie[3]

[1] Department of Mathematics, Faculty of Science, Jiangsu University, Zhenjiang 212013, China
[2] Department of Mathematics, COMSATS University Islamabad (CUI), 455000, Park Road, Tarlai Kalan, Islamabad, Pakistan
[3] Department of Mathematical Sciences, Faculty of Science, Universiti Teknologi Malaysia, 81310 UTM Johor Bahru, Johor 81310, Malaysia

E-mail: mqasim@ujs.edu.cn

Received 3 October 2019, revised 25 December 2019
Accepted for publication 25 December 2019
Published 24 February 2020

Abstract

In this article, three-dimensional mixed convection flow over an exponentially stretching sheet is investigated. Energy equation is modelled in the presence of viscous dissipation and variable thermal conductivity. Temperature of the sheet is varying exponentially and is chosen in a form that facilitates the similarity transformations to obtain self-similar equations. Resulting nonlinear ordinary differential equations are solved numerically employing the Runge–Kutta shooting method. In order to check the accuracy of the method, these equations are also solved using bvp4c built-in routine in Matlab. Both solutions are in excellent agreement. The effects of physical parameters on the dimensionless velocity field and temperature are demonstrated through various graphs. The novelty of this analysis is the self-similar solution of the three-dimensional boundary layer flow in the presence of mixed convection, viscous dissipation and variable thermal conductivity.

Keywords: self-similar equations, viscous dissipation, mixed convection, variable thermal conductivity, shooting technique, bvp4c Matlab

(Some figures may appear in colour only in the online journal)

1. Introduction

Flow induced by a continuously stretching sheet in a quiescent fluid have applications in manufacturing processes of plastic films, hot rolling, glass fiber, wire drawing, paper production, extrusion, spinning of laments, production of synthetic sheets, glass fiber and paper production, extrusion, continuous casting, spinning of laments, production of synthetic sheets etc [1–10]. In convection, there is a fluid flowing relative to surface and a temperature difference between fluid and surface. In these heat convection processes, energy is transferred from a surface to fluid flowing over it as a result of temperature difference between fluid and surface. The flow over a surface is also induced by thermal buoyancy and these thermal buoyancy effects are more prominent if the surface is vertical. When the sheet is being stretched vertically with a forced velocity then buoyance forces cannot be neglected and flow in this case is mixed convective flow [11–19].

Boundary layer flow over an exponentially stretching surface is firstly investigated by Magyari and Keller [20]. Elbashbeshy [21] performed heat transfer analysis of the flow induced by a permeable exponentially stretching sheet. Sajid and Hayat [22] computed the series solution of the self-similar equations that governs the flow over an exponentially stretching sheet in the presence of linear thermal radiation by the homotopy analysis method. The effect of thermal radiation in the presence of viscous dissipation on the flow over an exponentially stretching sheet is examined by Bidin and Nazar [23]. Partha *et al* [24] provided the similarity solution

[4] Author to whom any correspondence should be addressed.

of mixed convection flow over an exponentially stretching sheet in the presence of frictional heating. Bhattacharyya and Layek [25] investigated boundary layer flow over an exponentially stretching surface in an exponentially moving parallel free stream. Dual solutions of MHD boundary layer flow induced by an exponentially stretching sheet with non-uniform heat sink/source are analysed by Raju *et al* [26]. Sulochana and Sandeep [27] examined the stagnation point flow of nanofluid over an exponentially shrinking/stretching cylinder. Three-dimensional flow of viscous fluid over an exponentially stretching sheet is firstly studied by Liu *et al* [28]. Afridi and Qasim [29] inspected the entropy generation in three-dimensional boundary flow over an exponentially stretching surface in the presence of viscous dissipation.

All studies cited above related to flow induced by the exponentially stretching sheet with constant fluid properties. It is now well established that the physical properties of fluids may vary with temperature [30–34]. The magnitude of variation in properties varies from one fluid to another and depends on temperature limits of ambient fluid. It can be observed that the variable viscosity and thermal conductivity are quite significant for most of the fluids as compared to the variations in other properties. It is also believed that the difference between the theoretical and experimental results is because the properties of fluid are assumed to be constant and not temperature-dependent.

To best of our knowledge no one analysed the three-dimensional boundary layer flow over an exponentially stretching sheet with temperature-dependent thermal conductivity. Keeping this in mind, our aim is to analyse three-dimensional mixed convection flow induced by exponentially stretching sheet in the presence of frictional heating. The thermal conductivity of fluid is assumed to vary with temperature. Governing equations are modelled and simplified under boundary layer approximations. Modelled partial differential equations are then transformed into non-linear ordinary differential equations by utilizing similarity transformations. Special forms of stretching velocity and surface temperature varying exponentially are chosen for accurate similarity transformations. The novelty of the present study is the self-similar solution of three-dimensional boundary-layer flow in the presence of mixed convection, viscous dissipation and temperature-dependent thermal conductivity. To check the validation of our numerical code of the shooting method obtained results are also compared with Matlab boundary value solver bvp4c [35]. Effects of physical parameters of interest on velocity and temperature profile are analyzed.

2. Formulation

Three-dimensional mixed convection boundary layer flow over a sheet that is being stretched exponentially has been considered for investigation. The sheet is being stretched in both $x-$ and $y-$ directions with velocities $u_w = u_0 e^{\left(\frac{x+y}{L}\right)}$ and $v_w = v_0 e^{\left(\frac{x+y}{L}\right)}$ respectively. The temperature of the sheet is $T_s = T_a + Ae^{2\left(\frac{x+y}{L}\right)}$ (A is the constant characteristic temperature) and the temperature of the ambient fluid is T_a. In the presence of frictional heating the boundary layer equations for the flow and heat transfer are [28, 29]:

$$\frac{\partial u}{\partial x} + \frac{\partial v}{\partial y} + \frac{\partial w}{\partial z} = 0, \tag{1}$$

$$u\frac{\partial u}{\partial x} + v\frac{\partial u}{\partial y} + w\frac{\partial u}{\partial z} = \frac{\mu}{\rho}\frac{\partial^2 u}{\partial z^2} + g\alpha_T(T - T_a), \tag{2}$$

$$u\frac{\partial v}{\partial x} + v\frac{\partial v}{\partial y} + w\frac{\partial v}{\partial z} = \frac{\mu}{\rho}\frac{\partial^2 v}{\partial z^2}, \tag{3}$$

$$u\frac{\partial T}{\partial x} + v\frac{\partial T}{\partial y} + w\frac{\partial T}{\partial z} = \frac{1}{\rho S_p}\left[k(T)\frac{\partial^2 T}{\partial z^2} + \frac{\partial k(T)}{\partial T}\left(\frac{\partial T}{\partial z}\right)^2\right] + \frac{\mu}{\rho S_p}\left[\left(\frac{\partial u}{\partial z}\right)^2 + \left(\frac{\partial v}{\partial z}\right)^2\right], \tag{4}$$

along with physical boundary conditions [28, 29]

$$u(x, y, 0) = u_0 e^{\left(\frac{x+y}{L}\right)},\ v(x, y, 0) = v_0 e^{\left(\frac{x+y}{L}\right)},$$
$$w(x, y, 0) = 0,\ T(x, y, 0) = T_s = T_a + Ae^{2\left(\frac{x+y}{L}\right)}, \tag{5}$$

$$u(x, y, z \to \infty) \to 0,\ v(x, y, z \to \infty) \to 0,$$
$$T(x, y, z \to \infty) \to T_a, \tag{6}$$

where u, v and w are the components of velocity along $x-$, $y-$ and $z-$ axes, respectively, u_0 and v_0 are stretching parameters, μ is the dynamic viscosity, ρ is the density of fluid, g is the acceleration due to gravity, α_T is the thermal expansion coefficient, S_p denotes the specific heat, $k(T)$ is the thermal conductivity of the fluid, which is assumed to be temperature-dependent and take the following form [30–34]:

$$k(T) = k_a\left(1 + \delta\left(\frac{T - T_a}{T_s - T_a}\right)\right), \tag{7}$$

here δ is the variable thermal conductivity parameter.

Introducing similarity transformations

$$\xi = \sqrt{\frac{u_0}{2\nu L}}\, z e^{\left(\frac{x+y}{2L}\right)},\ u = u_0 e^{\left(\frac{x+y}{L}\right)} F'(\xi),$$
$$v = v_0 e^{\left(\frac{x+y}{L}\right)} G'(\xi),$$

$$w = -\sqrt{\frac{\nu u_0}{2L}}\, e^{\left(\frac{x+y}{2L}\right)}(F + \xi F' + G + \xi G'),$$
$$T = T_a + (T_s - T_a)\Theta. \tag{8}$$

With similarity variable ξ, F' and G' being the dimensionless axial and transverse velocities, respectively, Θ is the dimensionless temperature and prime denotes the differentiation with respect to ξ. Equations (1)–(4) along with boundary conditions (5) and (6) after using transformations (8) are transformed to self-similar equations

$$F''' + FF'' + GF'' - 2F'^2 - 2F'G' + 2\lambda\Theta = 0, \tag{9}$$

$$G''' + FG'' + GG'' - 2F'G' - 2G'^2 = 0, \tag{10}$$

$$(1 + \delta\Theta)\Theta'' + \delta\Theta'^2 + \Pr(F + G)\Theta' - 4\Pr(F' + G')\Theta + Ec\Pr(F''^2 + G''^2) = 0, \tag{11}$$

with boundary conditions

$$F(0) = 0, F'(0) = 1,$$
$$G(0) = 0, G'(0) = \varepsilon, \quad \Theta(0) = 1, \tag{12}$$
$$F'(\infty) = 0, G'(\infty) = 0, \quad \Theta(\infty) = 0.$$

Here $\varepsilon = \frac{u_0}{v_0}$ is velocity ratio parameter, $Ec = \frac{u_0^2}{S_p A}$ is Eckert number, and $Pr = \frac{\mu S_p}{k_a}$ is Prandtl number and $\lambda = \frac{Gr_x}{\mathrm{Re}_x^2} = \frac{gA\alpha_T L}{u_0^2}$ is the mixed convection parameter.

3. Solution methodologies

3.1. Shooting method

In order to solve self-similar non-linear equations (9)–(11) along with boundary conditions (11) are solved numerically by the Runge–Kutta shooting method, the boundary value problem is firstly converted into initial value problem by letting

$$e_1 = F, e_2 = e_1' = F', e_3 = e_2' = F'', e_4 = G, e_5 = e_4' = G', e_6 = e_5' = G'', e_7 = \Theta, e_8 = e_7' = \Theta'. \tag{13}$$

Incorporating equation (13) into equations (9)–(11), we get following system of first-order equations

$$\begin{pmatrix} e_1' \\ e_2' \\ e_3' \\ e_4' \\ e_5' \\ e_6' \\ e_7' \\ e_8' \end{pmatrix} = \begin{pmatrix} e_2 \\ e_3 \\ -e_1 e_3 - e_4 e_3 + 2e_2 e_2 + 2e_2 e_5 - 2\lambda e_7 \\ e_5 \\ e_6 \\ -e_1 e_6 - e_4 e_6 + 2e_5 e_5 + 2e_2 e_5 \\ e_8 \\ \frac{1}{1+\delta e_7}[4\mathrm{Pr}(e_2 + e_5)e_7 - \mathrm{Pr}(e_1 + e_4)e_8 - \mathrm{Pr}Ec(e_3 e_3 + e_6 e_6) - \delta e_8 e_8] \end{pmatrix}, \tag{14}$$

with initial conditions

$$\begin{pmatrix} e_1(0) \\ e_2(0) \\ e_3(0) \\ e_4(0) \\ e_5(0) \\ e_6(0) \\ e_7(0) \\ e_8(0) \end{pmatrix} = \begin{pmatrix} 0 \\ 1 \\ q_1 \\ 0 \\ \varepsilon \\ q_2 \\ 1 \\ q_3 \end{pmatrix}. \tag{15}$$

The shooting scheme is applied to find the missing initial conditions to guess q_1, q_2 and q_3 until the conditions $F'(\infty) = 0$, $G'(\infty) = 0$ and $\Theta(\infty) = 0$ are satisfied. After finding these missing conditions, the system of the first-order ordinary differential equation (14) is solved by the Runge–Kutta method.

3.2. Bvp4c

The numerical solutions are also computed by using Matlab built-in boundary value solver bvp4c. Matlab code bvp4c for the two-point boundary value problem is a finite difference code based on three-stage collocation at Lobatto points. These collocation polynomials provide a C^1-continuous solution, which is fourth order uniformly accurate in the interval of integration. Mesh selection and error control are based on the residual of the continuous solution. The collocation method routines a mesh of points to divide the interval of integration into subintervals. The solver computed a numerical solution by solving a global system of algebraic equations resulting from the boundary conditions and the collocation conditions imposed on all the subintervals. The solver then estimates the error of obtained numerical solution on each subinterval. The solver adapts the mesh and repeats the process, until the solution satisfies the tolerance criteria [35].

3.3. Code validation

The comparison between the shooting method and bvp4c is presented in table 1 for the validation of our numerical codes. Moreover, table 2 shows the comparison of present results with the existing study. The attained results are found to be in excellent agreement.

4. Results and discussion

The effects of mixed convection parameter λ, Prandtl number Pr Eckert number Ec, velocity ratio parameter ε and variable thermal conductivity parameter δ on velocity components $F'(\xi)$, $G'(\xi)$ and temperature $\Theta(\xi)$ are investigated. This purpose is achieved by plotting figures 1–9. The effect of the mixed convection parameter on velocity $F'(\xi)$ is seen in figure 1. Velocity $F'(\xi)$ increases by increasing λ. For large λ, there is a stronger buoyancy force due to which momentum boundary layer increases. The influence of Prandtl number Pr on velocity $F'(\xi)$ is displayed in figure 2. The large values of Prandtl number Pr correspond to stronger momentum and weaker thermal diffusivity, which therefore reduces the thermal boundary layer thickness. Figure 3 explicates the effect of Eckert number Ec on the velocity As expected velocity increases by increasing Ec. Figure 4 illustrates that velocity $F'(\xi)$ decreases by increasing velocity ratio parameter ε whereas velocity $G'(\xi)$ increases by increasing velocity ratio parameter ε (see figure 5). Temperature and

Table 1. Effects of different physical parameters on $F''(0)$, $-G''(0)$, $\Theta''(0)$ and comparison between shooting method and built-in routine bvp4c in Matlab.

					$-F''(0)$		$-G''(0)$		$-\Theta'(0)$	
λ	Pr	Ec	δ	ε	Shooting	bvp4c	Shooting	bvp4c	Shooting	bvp4c
0.0	1.2	0.6	0.2	0.5	1.569 89	1.569 62	0.784 94	0.784 75	1.823 65	1.823 55
0.5	1.2	0.6	0.2	0.5	1.271 68	1.271 24	0.806 53	0.806 12	1.932 93	1.932 77
1.0	1.2	0.6	0.2	0.5	0.996 57	0.996 18	0.823 76	0.823 45	2.015 22	2.015 09
1.5	1.2	0.6	0.2	0.5	0.735 65	0.735 44	0.838 61	0.838 36	2.080 27	2.080 11
1.2	**0.3**	0.6	0.2	0.5	0.591 71	0.591 49	0.865 19	0.864 87	1.007 37	1.007 23
1.2	**0.7**	0.6	0.2	0.5	0.773 96	0.773 64	0.843 76	0.843 42	1.556 59	1.556 41
1.2	**1.2**	0.6	0.2	0.5	0.890 79	0.890 47	0.829 93	0.829 78	2.042 99	2.042 81
1.2	**6.7**	0.6	0.2	0.5	1.171 19	1.170 98	0.803 08	0.802 73	4.752 33	4.752 02
1.2	1.0	**0.0**	0.2	0.5	0.892 27	0.892 06	0.829 71	0.829 65	2.033 36	2.033 22
1.2	1.0	**1.0**	0.2	0.5	0.827 28	0.826 95	0.837 35	0.837 19	1.760 31	1.760 17
1.2	1.0	**2.0**	0.2	0.5	0.771 27	0.771 13	0.843 79	0.843 52	1.524 76	1.524 61
1.2	1.0	**3.0**	0.2	0.5	0.722 07	0.721 95	0.849 35	0.849 14	1.316 99	1.316 71
1.2	1.0	0.5	**0.0**	0.5	0.887 74	0.887 55	0.830 98	0.830 65	2.129 88	2.129 69
1.2	1.0	0.5	**1.0**	0.5	0.765 63	0.765 48	0.843 08	0.842 88	1.375 84	1.375 77
1.2	1.0	0.5	**2.0**	0.5	0.683 16	0.683 03	0.852 15	0.851 94	1.081 84	1.081 69
1.2	1.0	0.5	**3.0**	0.5	0.622 25	0.622 11	0.859 14	0.858 92	0.916 69	0.916 52

Table 2. Comparison between our numerical results and the results of Liu *et al* [28] for $F''(0)$ and $G''(0)$ in the case where $\lambda = 0$, $\delta = 0$, $Ec = 0$.

	$-F''(0)$		$-G''(0)$	
ε	[28]	Present	[28]	Present
0.0	1.281 808 56	1.281 808 56	0.784 944 23	0.784 944 23
0.5	1.569 888 46	1.569 888 47	0.000 000 0	0.000 000 0
1.0	1.812 751 05	1.812 751 05	1.812 751 05	1.812 751 05

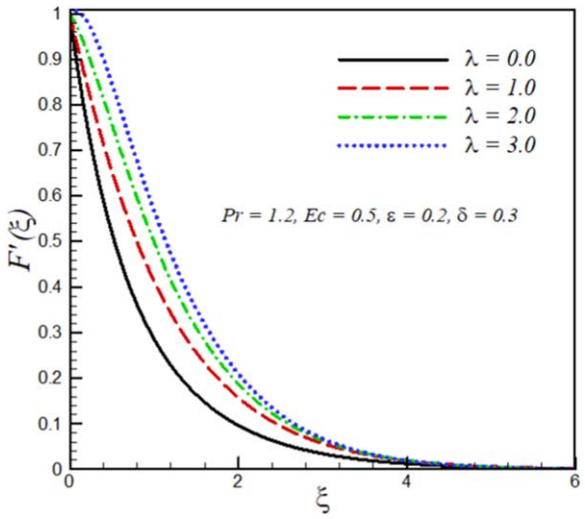

Figure 1. Effects of mixed convection parameter λ on velocity $F'(\xi)$.

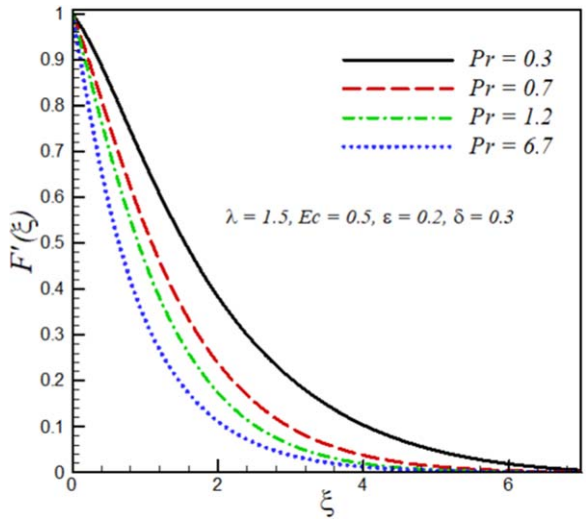

Figure 2. Effect of Prandtl number Pr on velocity $F'(\xi)$.

thermal boundary layer decreases upon increasing mixed convection parameter λ (see figure 6). Increasing the buoyancy parameter specifies the higher temperature from the surface relative to ambient, therefore thermal boundary layer decreases. The influence of Prandtl number Pr on the temperature field is illustrated in figure 7. The increase in the Prandtl number Pr indicates a reduction in the thermal conductivity of the fluid and because of this reduction, the penetration depth of the thermal energy decreases, therefore temperature of the fluid decreases. Figure 8 shows that temperature distribution and thermal boundary layer thickness increases with an increase in Eckert number Ec. Physically, by increasing friction between the adjacent layers of fluid increases and the kinetic energy of fluid is converted into

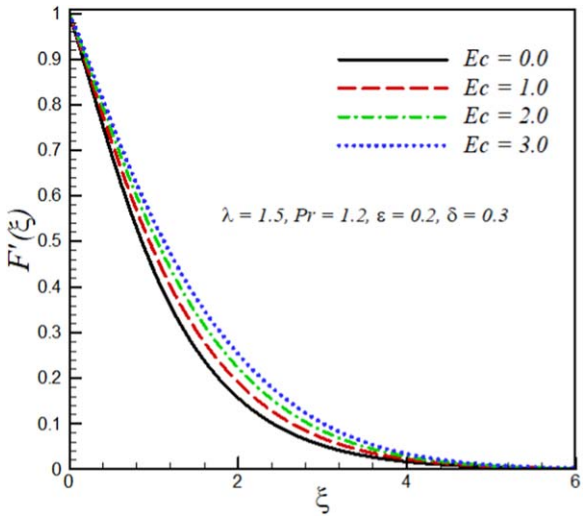

Figure 3. Effect of Eckert number Ec on velocity $F'(\xi)$.

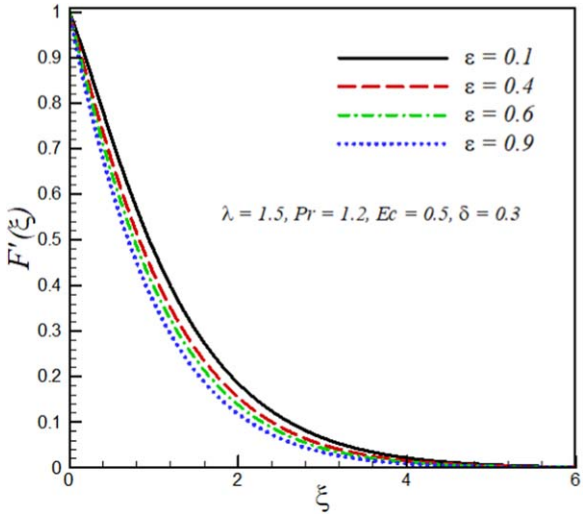

Figure 4. Effect of velocity ratio parameter ε on velocity $F'(\xi)$.

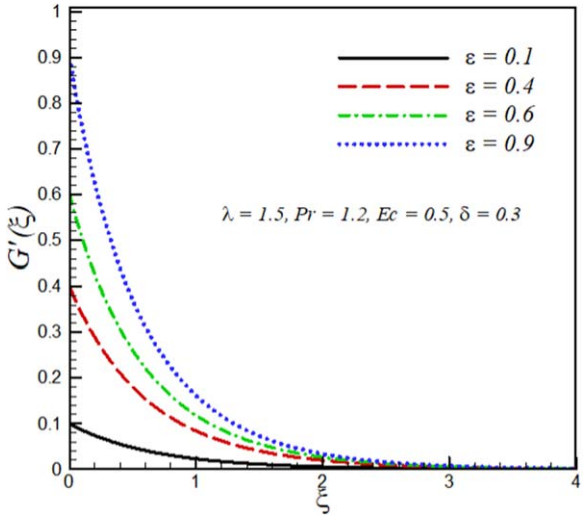

Figure 5. Effect of velocity ratio parameter ε on velocity $G'(\xi)$.

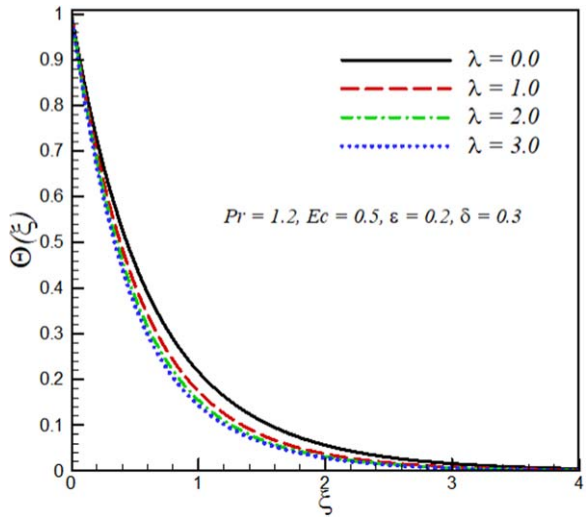

Figure 6. Effect of mixed convection parameter λ on temperature profile $\Theta(\xi)$.

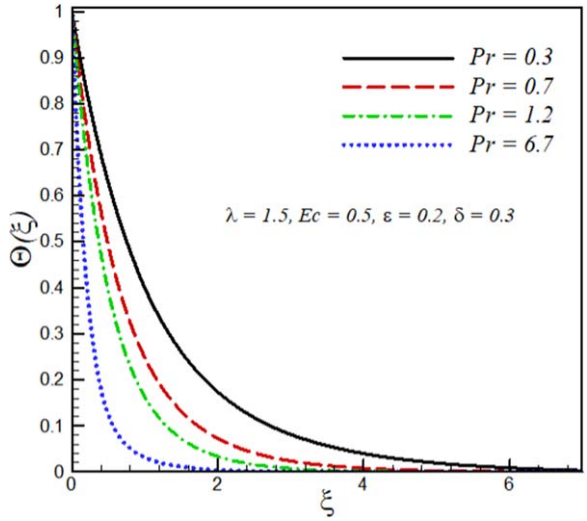

Figure 7. Effect of Prandtl number Pr on temperature profile $\Theta(\xi)$.

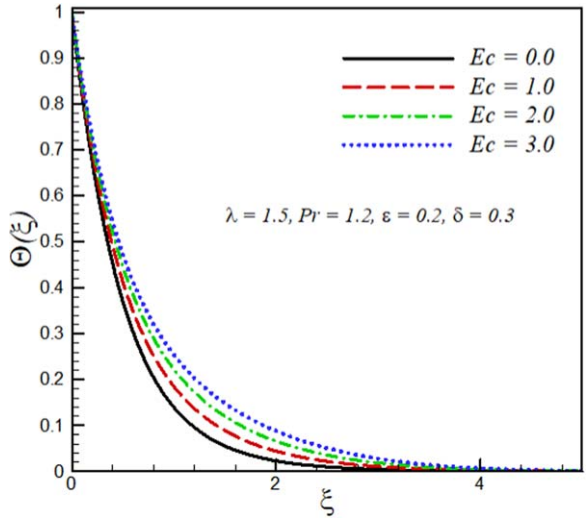

Figure 8. Effect of Eckert number Ec on temperature profile $\Theta(\xi)$.

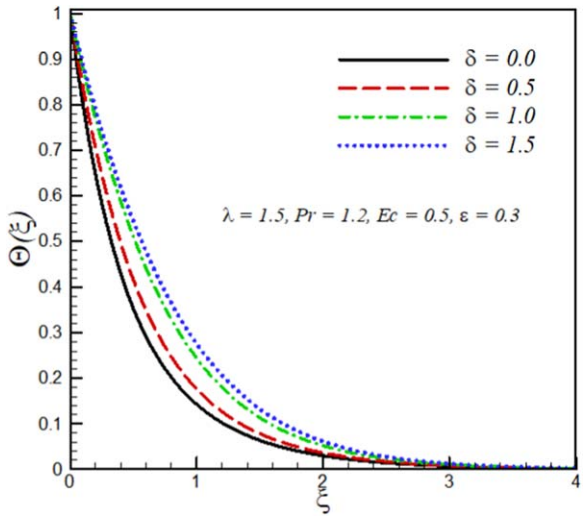

Figure 9. Effect of variable thermal conductivity parameter δ on temperature profile $\Theta(\xi)$.

thermal energy, which in turn rises the fluid temperature. The influence of the thermal conductivity parameter δ on the temperature profile is portrayed in figure 9. It is observed that the temperature of the fluid in the boundary layer increases by increasing the value of the variable thermal conductivity parameter δ. Physically, as the thermal conductivity parameter increases, the thermal conductivity of the fluid increases and, as a result, the thermal energy of fluid increases, resulting in an increase in temperature. Table 1 shows that skin friction coefficients along $-F''(0)$ transverse direction decreases by increasing mixed convection parameter λ, whereas $-G''(0)$ and local Nusselt number $-\Theta'(0)$ increases with increasing mixed convection parameter λ. Skin friction coefficients and local Nusselt number decreases by increasing the variable thermal conductivity parameter. $-F''(0)$ and $-\Theta'(0)$ are decreasing functions of Eckert number Ec whereas increasing functions of Prandtl number Pr.

5. Closing remarks

From the current analysis, the following specific conclusions are deduced:

- The problem is self-similar in the presence mixed convection as well as viscous dissipation for a special type of surface temperature.
- The mixed convection parameter increases the velocity profile, but it decreases the temperature profile in the boundary layer region.
- Velocity component F' in the transverse direction and dimensionless temperature Θ decreases by increasing the Prandtl number, whereas both are decreasing functions of the Eckert number.
- Velocity decreases F' whereas G' increases by increasing the velocity ratio parameter.
- Temperature profile increases by increasing the variable thermal conductivity parameter.

References

[1] Salleh M Z, Nazar R and Pop I 2010 Boundary layer flow and heat transfer over a stretching sheet with Newtonian heating *Journal of Taiwan Institute of Chemical Engineering* **41** 651–5
[2] Turkyilmazoglu M 2011 Analytic heat and mass transfer of the mixed hydrodynamic/thermal slip MHD viscous flow over a stretching sheet *Int. J. Mech. Sci.* **53** 886–96
[3] Makinde O D and Aziz A 2011 Boundary layer flow of a nanofluid past a stretching sheet with a convective boundary condition *Int. J. Therm. Sci.* **50** 1326–32
[4] Turkyilmazoglu M and Pop I 2013 Exact analytical solutions for the flow and heat transfer near the stagnation point on a stretching/shrinking sheet in a Jeffrey fluid *Int. J. Heat Mass Transfer* **57** 82–8
[5] Sheikholeslami M and Ganji D D 2014 Heated permeable stretching surface in a porous medium using nanofluids *Journal of Applied Fluid Mechanics* **7** 535–42
[6] Khan W A and Makinde O D 2014 MHD nanofluid bioconvection due to gyrotactic microorganisms over a convectively heat stretching sheet *Int. J. Therm. Sci.* **81** 118–24
[7] Rashidi M M, Abdul A K, Hakeem, Vishnu N, Ganesh, Ganga B, Sheikholeslami M and Momoniat E 2016 Analytical and numerical studies on heat transfer of a nanofluid over a stretching/shrinking sheet with second-order slip flow model *International Journal of Mechanical and Materials Engineering* **11** 1–9
[8] Hsiao K L 2017 Micropolar nanofluid flow with MHD and viscous dissipation effects towards a stretching sheet with multimedia feature *Int. J. Heat Mass Transfer* **112** 983–90
[9] Rashidi M M and Abbas M A 2017 Effect of slip conditions and entropy generation analysis with an effective Prandtl number model on a nanofluid flow through a stretching sheet *Entropy* **19** 414
[10] Turkyilmazoglu M 2017 Magnetohydrodynamic two-phase dusty fluid flow and heat model over deforming isothermal surfaces *Phys. Fluids* **29** 013302
[11] Chamkha A J and Issa C 1999 Mixed convection effects on unsteady flow and heat transfer over a stretched surface *Int. Commun. Heat Mass Transfer* **26** 717–28
[12] Hsiao K L 2008 MHD mixed convection of viscoelastic fluid over a stretching sheet with Ohmic dissipation *Journal of Mechanics* **24** 29–34
[13] Prasad K V, Vajravelu K and Datti P S 2010 Mixed convection heat transfer over a non-linear stretching surface with variable fluid properties *Int. J. Non Linear Mech.* **45** 320330
[14] Turkyilmazoglu M 2013 The analytical solution of mixed convection heat transfer and fluid flow of a MHD viscoelastic fluid over a permeable stretching surface *Int. J. Mech. Sci.* **77** 263–8
[15] Ellahi R, Hassan M and Zeeshan A 2016 Aggregation effects on water base Al2O3–nanofluid over permeable wedge in mixed convection *Asia-Pac. J. Chem. Eng.* **11** 179–86
[16] Sheikholeslami M, Mustafa M T and Ganji D D 2016 Effect of Lorentz forces on forced convection nanofluid flow over a stretched surface *Particuology* **26** 108–13
[17] Ellahi R, Hassan M and Zeeshan A 2017 Shape effects of spherical and nonspherical nanoparticles in mixed convection flow over a vertical stretching permeable sheet *Mech. Adv. Mater. Struct.* **24** 1231–8
[18] Afridi M I, Qasim M, Khan I, Shafie S and Alshomrani A S 2017 Entropy generation in magnetohydrodynamic mixed convection flow over an inclined stretching sheet *Entropy* **19** 1–11
[19] Turkyilmazoglu M 2018 Analytical solutions to mixed convection MHD fluid flow induced by a nonlinearly

deforming permeable surface *Commun. Nonlinear Sci. Numer. Simul.* **63** 373–9
[20] Magyari E and Keller B 1999 Heat and mass transfer over an exponentially stretching continuous surface *J. Phys. D: Appl. Phys.* **32** 577–85
[21] Elbashbeshy E M A 2001 Heat transfer over an exponential stretching continuous surface with suction *Arch. Mech.* **53** 643–51
[22] Sajid M and Hayat T 2008 Influence of thermal radiation on the boundary layer flow due to an exponentially stretching sheet *Int. Commun. Heat Mass Transfer* **35** 347–56
[23] Bidin B and Nazar R 2009 Numerical solution of the boundary layer flow over an exponentially stretching sheet with thermal radiation *European Journal of Scientific Research* **33** 710–7
[24] Partha M K, Murthy P V S N and Rajasekhar G P 2005 Effect of viscous dissipation on mixed convection heat transfer from an exponentially stretching surface *Heat Mass Transfer* **41** 360–6
[25] Bhattacharyya K and Layek G C 2014 Thermal boundary layer in flow due to an exponentially stretching surface with an exponentially moving free stream *Modelling and Simulation in Engineering* **2014** 785049
[26] Raju C S K, Sandeep N, Sulochana C and Babu M J 2016 Dual solutions of MHD boundary layer flows pas an exponentially stretching sheet with non-uniform heat source/sink *Journal of Applied Fluid Mechanics* **9** 555–63
[27] Sulochana C and Sandeep N 2016 Stagnation point flow and heat transfer behavior of Cu- water nanofluid towards horizontally and exponentially stretching/shrinking cylinder *Applied Nanosciences* **6** 108–13
[28] Liu I C, Wang H H and Peng Y F 2013 Flow and heat transfer for three-dimensional flow over an exponentially stretching surface *Chem. Eng. Commun.* **200** 253–68
[29] Qasim M and Afridi M I 2018 Effects of energy dissipation and variable thermal Conductivity on entropy generation rate in mixed convection flow *Journal of Thermal Science and Engineering Applications* **10** 044501
[30] Chaim T C 1998 Heat transfer in a fluid with variable thermal conductivity over stretching sheet *Acta Mech.* **129** 63–72
[31] Chaim T C 1996 Heat transfer with variable conductivity in a stagnation-point flow towards a stretching sheet *Int. Commun. Heat Mass Transfer* **23** 239–48
[32] Prasad K V, Vajravelu K and Datti P S 2010 Mixed convection heat transfer over a non-linear stretching surface with variable fluid properties *Int. J. Non Linear Mech.* **45** 320–30
[33] Hayat T, Shehzad S A, M Qasim and Alsaedi A 2014 Mixed convection flow by a porous sheet with variable thermal conductivity and convective boundary condition *Braz. J. Chem. Eng.* **31** 1–13
[34] Hussain Q, Asghar S, Hayat T and Alsaedi A 2015 Heat transfer analysis in peristaltic flow of mhd jeffrey fluid with variable thermal conductivity *J. Appl. Math. Mech.* **9** 015–1926
[35] Kierzenka J and Shampine L F 2001 A BVP solver based on residual control and the MATLAB PSE *ACM Transactions in Mathematics and Software* **27** 299–316